J. Fluid Mech. (1984), *vol.* 145, *pp.* 339–360
Printed in Great Britain

Turbulent flow with heat transfer in plane and curved wall jets

By T. DAKOS, C. A. VERRIOPOULOS AND M. M. GIBSON
Fluids Section, Mechanical Engineering Department, Imperial College of Science and Technology, Exhibition Road, London SW7 2BX

(Received 27 October 1983 and in revised form 11 April 1984)

Extensive single-point turbulence measurements made in a heated wall jet on a convex wall, and in an equivalent plane flow, show that the turbulence structure and the transfer of heat and momentum are affected by wall curvature. In the curved wall jet the points of zero shear stress and zero streamwise heat flux are displaced further from the point of maximum velocity, the Stanton number for heat transfer from the surface is reduced more than the skin-friction coefficient, and temperature profiles in the inner layer depart from the flat-flow wall law. The shear stress, turbulent intensities and turbulent heat fluxes are reduced by stabilizing curvature in the inner layer and increased by destabilizing curvature in the outer flow. The largest changes occur in the triple products, which are nearly doubled by destabilizing curvature.

1. Introduction

The paper deals with heat transfer through two related two-dimensional complex turbulent shear layers: a wall jet in an external stream on a heated plane surface, and the corresponding flow on a mildly curved convex surface. Our interest in this topic stems from an early attempt by Gibson (1978) to apply the well-known analogy between buoyancy and streamline curvature to predict the effects of curvature on heat transfer. At that time it was discovered that there were no measurements available to prove or disprove the prediction that heat transfer is less sensitive to the effects of curvature than momentum transfer. We have since made measurements in a boundary layer on a heated convex plate (Gibson, Verriopoulos & Nagano 1982; Gibson & Verriopoulos 1984; Gibson, Verriopoulos & Vlachos 1984) which show that a step change in wall curvature has exactly the opposite effect. The present study is the sequel to our boundary-layer experiment, extended here to a more complex flow.

The wall jet may be thought of as a composite flow made up of two interacting shear layers: an inner layer possessing many of the characteristics of an ordinary turbulent boundary layer, and an outer layer which, though influenced by the presence of the wall, is broadly similar in its structure to a free mixing layer. The best known and most remarkable result of the interaction in this flow is that the point at which the shear stress changes sign does not coincide with the position of the zero velocity gradient but lies inside it, closer to the wall. When a wall jet develops on a convex surface the turbulence is stabilized in the inner layer and destabilized in the outer. Changes in the shear stress and turbulent intensities accord with the general rule (Bradshaw 1973) that these are an order of magnitude greater than the ratio of shear-layer thickness to the radius of curvature. The position of zero shear stress moves further from the position of the velocity maximum.

Because it is such an interesting flow, a degree more complex than a boundary layer yet relatively easy to set up in the laboratory, and because it is important in engineering practice with applications in film cooling and advanced aerofoil design, the wall jet has received considerable attention from experimenters and modellers. Launder & Rodi (1981), in a survey carried out for the recent AFOSR–Stanford Conferences on Complex Turbulent Shear Flows, discovered over two hundred experimental studies, of which over seventy were critically examined as possible test cases for the evaluation of calculation methods. It was found, however, that in only a few cases were measurements made in sufficient detail to be useful for this purpose; seven of these concerned wall jets on convex walls. The authors identified a number of gaps and inconsistencies in the data, thus: 'turbulence measurements for wall jets in a uniform velocity stream are fairly scarce' and again 'only a few experimenters have measured all the Reynolds-stress components and among the available sets of data there is considerable scatter. There is virtually nothing reported on higher-moment correlations. . . ' Some, at least, of these measurements have been made in the course of the present study. That they are scarce is one reason for including them in a paper concerned mainly with heat transfer; another reason is that heat-transfer measurements in turbulent flows are on their own of little use, except in that they may provide specific answers to specific problems. It is unfortunate that the failure to provide adequate details of the velocity field so restricts the usefulness of the hundred papers alluded to by Launder & Rodi that deal explicitly with heat transfer.

The reader is referred to the Launder & Rodi (1981) survey for an account of previous work on wall jets in moving external streams, and on curved walls. Thirteen papers describe mean flow and a few turbulence measurements in the former that were sufficiently detailed to satisfy the survey criteria; of these, three are concerned with self-preserving wall jets in streamwise pressure gradients which maintain a constant ratio of maximum to free-stream velocity. The work of Irwin (1973) in particular contains very detailed and consistent measurements in a self-preserving flow with the velocity ratio 2.65. The other ten papers cited in the survey contain results from numerous investigations of wall jets in constant-velocity streams which are not self-preserving because the velocity ratio falls as the jet spreads. The rate of growth of the inner layer, defined by the distance of the maximum-velocity point from the wall, is a weak function of Reynolds number, but apparently independent of the initial velocity ratio, which, in these flows, ranged from about two to ten. The jet width to the half-velocity point (figure 1) scales on the local momentum thickness. It has been noted that turbulence measurements in wall jets of this type are fairly scarce. Kruka & Eskinazi (1964) have measured longitudinal fluctuations and shear stress, and Kacker & Whitelaw (1971) have measured all the non-zero stress components at one station. We have not considered here a number of data sets from blown boundary layers, which are not strictly comparable because the structure and development of the jet is affected by the character and history of a thick external boundary layer on the slot lip, which results in a wake with a velocity minimum in the downstream flow.†

The most extensive measurements of wall jets on convex surfaces are probably those of Guitton & Newman (1977) in the self-preserving flow on a logarithmic spiral, and Alcaraz (1977) in a constant-curvature flow. There was no free stream in either case. The effects of wall curvature recorded by Alcaraz are qualitatively in line with expectations. The flow developed on 16° of a convex wall of radius equal to 322 slot

† A referee has drawn our attention to the extensive turbulence measurements by Saripalli & Simpson (1980), which fall into this category.

heights; measurements were made at slot Reynolds numbers of 1.1×10^4 and 4×10^4 (the corresponding figures for the present flow with non-zero free stream are 24°, 222 and 3×10^4). At the higher Reynolds number the turbulence intensities and shear stress in the destabilized outer layer increased with distance downstream to levels significantly greater than those recorded in self-preserving plane flow. Consequently the spreading rate also increased with distance along the plate to a value about 25 % greater than that of a comparable plane layer. At the same time, the stabilizing effects of wall curvature in the inner layer caused the position of zero shear stress to move away from the velocity maximum and closer to the wall.

Although the literature contains a number of accounts of detailed measurements in heated plane wall boundary layers, and a few less-detailed studies of heat transfer through wall jets, the effects of wall curvature on boundary-layer heat transfer have received surprisingly little attention, while measurements in heated curved wall jets appear not to exist. The paper by Nizou (1981) may be taken as representative of the small number of papers on the heated wall jet: it contains mean-temperature profiles, a limited amount of information on the mean-velocity field and skin friction taken from Tailland (1970), and no turbulence measurements. The effects of wall curvature on heat transfer in boundary layers were investigated by Kreith (1955), Thomann (1968) and, more recently, by Mayle, Blair & Kopper (1979). These studies showed that changes in the Stanton number in curved wall flow were of the same order of magnitude as estimated changes in the skin-friction coefficient, which was not measured. As a first approximation, Reynolds' analogy might be assumed to be unaffected by curvature, or alternatively that the eddy-diffusivity ratio (the turbulent Prandtl number) remains the same as in plane flow. Assumptions of this nature may suffice for engineering calculations, but they are insecurely based. Examination of the boundary-layer equations for the shear stress $\overline{uv}$ and the heat flux $\overline{v\theta}$ (Appendix A) shows that the terms containing the extra strain rate of curved flow, $\partial V/\partial x \approx -U/r$, are weighted differently in the two equations with respect to the main generation terms. There is thus no reason to expect that these two quantities are affected in exactly the same way by curvature. Appeal to the buoyancy–curvature analogy (Bradshaw 1969) also undermines simple assumptions of the Reynolds' analogy description: the eddy-diffusivity ratio in density-stratified shear flow is known to be sensitive to the degree of stratification.

The results of two recent boundary-layer experiments confirm the view that heat and momentum transport respond in different ways to the introduction of wall curvature. Simon & Moffat (1979) (also Simon *et al.* 1980) measured surface heat fluxes and mean-temperature profiles in a heated boundary layer of thickness δ which developed first on a plane heated wall before being turned through a 90° bend of radius R. The sense of the curvature was stabilizing with $\delta/R \approx 0.10$, and strong enough to extinguish and reverse the sign of the shear stress in the outer part of the layer. At the end of the curved wall the Stanton number was approximately 30–40 % below the value that would be expected on a plane wall; the corresponding fall in the skin-friction coefficient was 30 %. An important finding was that, while the velocity profiles could be fitted satisfactorily to the law of the wall with the usual flat-plate constants, the temperature profiles deviated significantly from the corresponding temperature wall law.

Our own measurements, described by Gibson *et al.* (1982, 1984) and Gibson & Verriopoulos (1984), were made in a more mildly curved heated boundary layer for which $\delta/R \approx 0.01$. The Stanton number and skin-friction coefficient were depressed in the curved wall flow by 18 % and 12 % from their estimated plane-flow values. As

in the Simon & Moffat experiment, the velocity profiles were fitted satisfactorily by the law of the wall, but the temperature profiles were not, although for this mild curvature they retained a semi-logarithmic shape. The ratio κ/κ_θ, which is roughly equivalent to the eddy-diffusivity ratio or turbulent Prandtl number for the near-wall region, increased from 0.85 in the plane flow upstream of the bend to 1.03 when the flow had been turned through 30°. The effects of stabilizing curvature on turbulent diffusion were very striking: hot-wire and resistance-thermometer measurements showed that the triple products were halved in the curved layer.

The results of the present wall-jet experiments are broadly consistent with the results of the boundary-layer study. The skin-friction coefficients in the curved wall jet fall slightly below those of the equivalent plane flow, and the reduction in Stanton number is greater. The velocity profiles near the wall fit the universal law of the wall in both plane and curved flows. The logarithmic region of the temperature profile is gradually eroded in the curved wall jet until at the last traverse station, nearly 100 slot widths downstream of the slot, the profiles show a 20 % increase in slope in the inner layer. The most marked effects of curvature are on the triple products associated with the transport of Reynolds stress and heat flux. In the destabilized outer layer these quantities are substantially increased; in the inner layer they are reduced by roughly the amount obtained by scaling the corresponding changes in the boundary layer on δ/R.

The paper contains the results of pressure-tube and hot-wire measurements of mean velocity, the four non-zero components of the Reynolds-stress tensor and three triple-velocity products in a plane and in a curved wall jet, and of the surface heat fluxes, mean temperatures and corresponding double and triple velocity–temperature products. It is believed that these are the most extensive turbulence measurements yet attempted in a flow of this type. The implications of the results for future turbulence modelling are considered. Because we find the conservation equations are invaluable aid to the interpretation of curved-flow data, and because the heat-flux equations are not easily found in the literature, we have listed these in Appendix A. The overall conservation of momentum and enthalpy in the two flows is dealt with in Appendix B.

2. Experimental arrangements

The arrangement was largely conditioned by the availability of components and equipment used in the heated boundary-layer experiments cited in §1. There existed two 305×102 mm^2 wind tunnel sections 1.22 m in length, one straight and one curved to a mean radius of 2.49 m. The section floors, on which the test boundary layers developed, were made of 12.5 mm thick aluminium and were drilled for static pressure taps and miniature surface heat-flux meters as described by Gibson *et al.* (1982). These surfaces were heated by electric blankets. In these sections it was desired to produce wall jets under the wind tunnel free stream which would be thick enough to permit exploration with triple-wire probes but not so thick as to absorb the external potential flow and fill the section. After examination of existing data, and some preliminary experimentation, the slot height b was fixed at 11 mm and the ratio U_∞/U_j of free-stream to jet velocity at 0.57 (the notation is explained in figure 1). The velocity U_j in the plane of the slot was held constant at 41.3 m/s; the corresponding slot Reynolds number was 3×10^4.

The wall jet was generated in the short contracting section shown diagrammatically in figure 1. This section was bolted to the contraction of the open-circuit blower wind

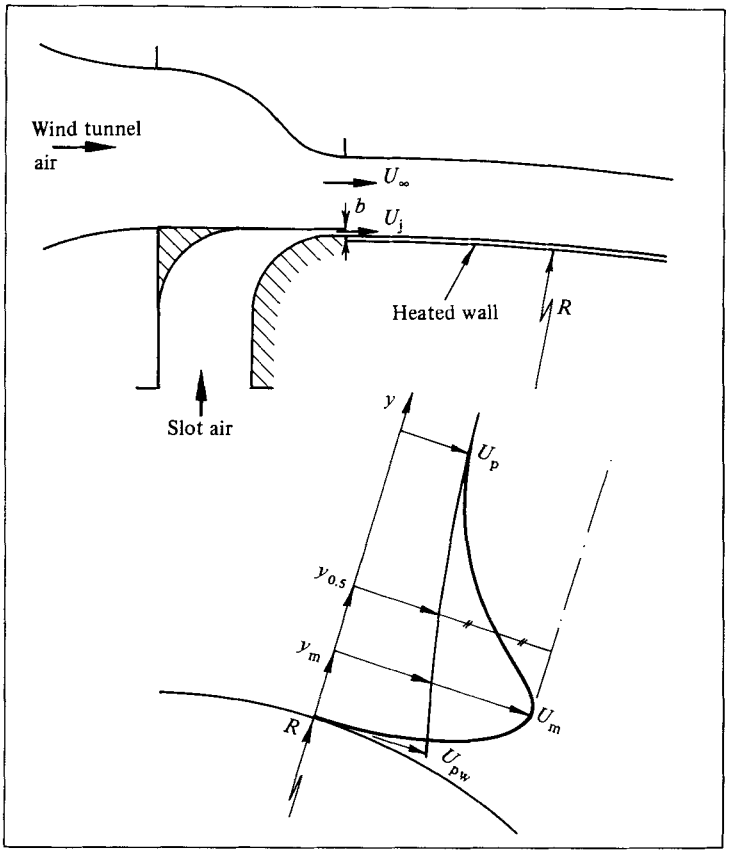

FIGURE 1. Experimental arrangement and nomenclature.

tunnel used in the previous experiments. The tunnel contraction ratio was thereby increased to 20:1. The slot air, which was supplied independently by a 1 h.p. centrifugal fan, passed through two honeycombs and four screens before entering the 11:1 contraction shown in figure 1 upstream of the slot. The turbulence in a mixing layer is known to be sensitive to the initial conditions set at the splitter plate, which in this case was a 1.5 mm thick mild-steel plate. We gave some thought to these conditions before deciding to follow Bradshaw's (1966) advice and leave the external boundary layer untripped. The boundary layer on the outside of the splitter plate was then approximately 1.5 mm thick with a shape factor of about 2. Inside the slot the boundary layers were approximately 1 mm thick, the central core was uniform to within 0.5 % and the ratio of maximum to mean velocity was approximately 1.05. We were unable to detect any spanwise variation of stagnation tube readings in the flow on either side of the splitter plate. The turbulence intensity in the free stream was 0.4 %.

The mixing layer between the two streams impinged on the flat plate 380 mm, and on the curved plate 340 mm, from the plane of the slot. From these points the plane and curved wall jets spread to thicknesses $y_{0.5}$ (defined in figure 1) of respectively 25 and 30 mm 93 slot heights (102 cm) from the slot. The streamwise variation in static pressure recorded at the wall tappings was small: over the range $46 < x < 102$ cm in which detailed measurements were made the free-stream velocity increased by only 2 %. In neither case was the flow self-preserving: this condition was

neither expected nor, indeed, desired. A flat wall jet requires a tailored pressure gradient for self-preservation (Irwin 1973) and a curved wall jet a wall curved in a logarithmic spiral (Guitton & Newman 1977). It seemed probable that one result of trying to meet these requirements would be to obscure the changes due to curvature that we wanted to observe. Both flows were thus allowed to develop gradually over the full lengths of the two plates with a nominally uniform free-stream velocity.

The aluminium floors of the two test sections were heated by electric blankets to a mean temperature 12 °C above that of the free stream. The maximum local variations from the mean recorded by copper–constantan thermocouples embedded in the plates was less than ± 0.5 °C. The temperatures of the two airstreams in the tunnel were equalized to within ± 0.2 °C by preheating the flow to the slot with a 1 kW electric fan heater carefully positioned at the blower intake. The temperature differences in the flow were small enough to allow the temperature to be considered as a passive scalar.

Surface heat-transfer measurements were made using three interchangeable 9.4 mm diameter heat-flux meters of the Schmidt–Boelter multiple-thermocouple type. These meters have linear characteristics with a sensitivity of 40 mV W^{-1} cm^2, and in these experiments an output of about 5 mV, which was measured on a Datron 1065A digital voltmeter to an estimated overall accuracy of $\pm 2\%$. Standard techniques were used for probe measurements in the flow. Mean velocities were calculated from stagnation-tube measurements using the followng equation for curved shear flow:

$$\tfrac{1}{2}\rho U^2 = \frac{P_\infty - p_w}{(1+y/R)^2} - (P_\infty - P),$$

in which P_∞ and P are the free-stream and local stagnation pressures and p_w is the static pressure measured at the wall. The shear stress at the wall was obtained by the Clauser method of fitting the mean-velocity profiles to the supposed universal law of the wall with the usual constants $\kappa = 0.41$ and $A = 5.0$. Mean temperatures were measured with a 12 μm diameter chromel–alumel thermocouple sensor welded to a standard miniature hot-wire probe. Turbulence measurements were made using 5 μm diameter hot wires fitted to miniature probes in a dual-channel DISA 55M01 constant-temperature anemometer. The hot-wire signals were linearized and processed digitally in the on-line microcomputer system described in detail by Verriopoulos (1983). Measurements of the temperature–velocity products were made using a three-wire probe in which a 1 μm 50 Ω cold resistance-thermometer wire, operated at low overheat, was independently mounted and positioned in the plane between the hot wires of an X-probe. Additional measurements of $\overline{u^2}$, $\overline{\theta^2}$ and $\overline{u\theta}$ were also obtained from a parallel twin-wire probe as a check on the three-wire results. These checks, supplemented by single-wire measurements of $\overline{u^2}$, showed no traces of the effects of mutual wire interference or temperature contamination of the hot-wire signals.

3. Results

3.1. *Main features of the flow*

The principal results of mean-velocity, temperature and surface-flux measurements are summarized in table 1 in the notation of figure 1. The velocity of the external potential flow, $U_p r$ = constant, evaluated at the wall replaces the free-stream velocity as a reference velocity for the curved wall jet. The pressure at the wall,

	x (cm)	Symbol	$\frac{U_{pw}}{U_j}$	$\frac{U_m}{U_j}$	$y_{0.5}$ (mm)	$\frac{y_{0.1}}{y_{0.5}}$	$\frac{y_m}{y_{0.5}}$	$\frac{y_s}{y_{0.5}}$	$c_f \times 10^3$	$\frac{y_\theta}{y_{0.5}}$	$St \times 10^3$
Flat	46	○	0.556	0.863	15.3	1.50	0.354	0.335	4.65	0.267	2.09
	76	□	0.561	0.774	20.3	1.47	0.393	0.360	4.40	0.315	2.01
	102	△	0.567	0.734	24.6	1.45	0.407	0.395	4.27	0.362	1.86
Curved	46	●	0.569	0.865	16.3	1.53	0.395	0.265	4.66	0.344	1.90
	76	■	0.572	0.780	24.0	1.49	0.410	0.275	4.33	0.342	1.84
	102	▲	0.578	0.738	30.1	1.47	0.419	0.300	4.09	0.349	1.68

TABLE 1. Main flow details

$p_w = P_\infty - \frac{1}{2}\rho U_{pw}^2$, is effectively constant for both flows. The thickness $y_{0.5}$, which has often been used previously as a measure of the wall-jet thickness, is redefined for the curved wall jet as the distance from the wall at which the velocity difference $U - U_p$ is equal to $\frac{1}{2}(U_m - U_p)$, where U_m is the maximum velocity and $U_p(r)$ is evaluated at $y = y_{0.5}$. Similarly $y_{0.1}$ is the distance from the wall to the point where $U - U_p = 0.1(U_m - U_p)$. y_m and y_s are the distances from the wall to the positions of maximum velocity and zero shear stress respectively, and the temperature-layer thickness y_θ is the distance to the point where $T - T_\infty = 0.1(T_w - T_\infty)$. The skin-friction coefficient c_f and the Stanton number St are both defined with respect to the maximum velocity.

The rates of growth with x of the different layer thicknesses given in table 1 are approximately linear and consistent with the results of previous measurements contained in the Launder & Rodi (1981) survey. The curved wall jet spreads more rapidly than the plane flow: $\mathrm{d}y_{0.5}/\mathrm{d}x$ is increased by 47 % and the growth rate of the destabilized outer layer, $\mathrm{d}(y_{0.1} - y_s)/\mathrm{d}x$, by nearly 90 %. A feature of the convex wall jet which has been remarked upon by Launder & Rodi is that the position y_m of maximum velocity increases more rapidly than in plane flow, in the present case by some 30 %. The point y_s of zero shear stress, which is about $0.95y_m$ in the plane wall jet, moves relatively nearer to the wall in the curved flow to approximately $0.7y_m$. The temperature layers are very much internal layers: the values of y_θ in table 1 show that over 90 % of the temperature change from the wall is effected in the inner layer inboard of the velocity maxima. In the plane wall jet y_θ/y_m increases from 0.75 at $x = 46$ cm to 0.89 at $x = 102$ cm; in the curved flow the corresponding values are 0.87 and 0.83. Changes in the fluctuating temperature field to be discussed later resemble those of the velocity field in the stably curved inner layer: the position of zero heat flux $\overline{u\theta}$ almost coincides with y_s in both flows and is displaced inwards in the curved wall jet.

Values of the skin-friction coefficient in the curved wall jet are consistent with the general rule that changes in this quantity relative to plane flow are an order of magnitude greater than the ratio of shear-layer thickness to radius of curvature: at the last measurement position $y_m/R = 0.0052$ and c_f is 3 % lower than the corresponding flat-plate value. This behaviour is very much as expected from previous boundary-layer and wall-jet experiments: c_f falls gradually along the curved wall, and the reduction below the corresponding flat-plate values increases with distance downstream. The observed effect of wall curvature on the Stanton number is much greater: at each of the three traverse positions of table 1 the curved-wall values are some 10 % lower than those on the flat plate. Moreover the change in St takes place further upstream, so that it is already apparent at the first traverse position, where the skin-friction coefficient is only slightly lower than that on the flat wall. Heat-flux measurements made at five intermediate positions confirm the trend shown by the three values of Stanton number quoted in table 1. The spread in the surface-meter readings is lower than the changes recorded: departures from the best-fit curve through the data do not exceed about 3 %.

Profiles of the mean velocity in the two wall jets, which are plotted in outer-layer coordinates in figure 2, show gradual streamwise development in the outer layers accompanied by slight changes in shape and dimensions resulting from the effects of destabilizing curvature. The mean flow in the inner layers is not scaled in these coordinates, as the ratio $(U_m - U_p)/U_{pw}$ decreases as the flows develop downstream, and values of $U < U_p$ are not shown. The profiles plotted in wall-law coordinates

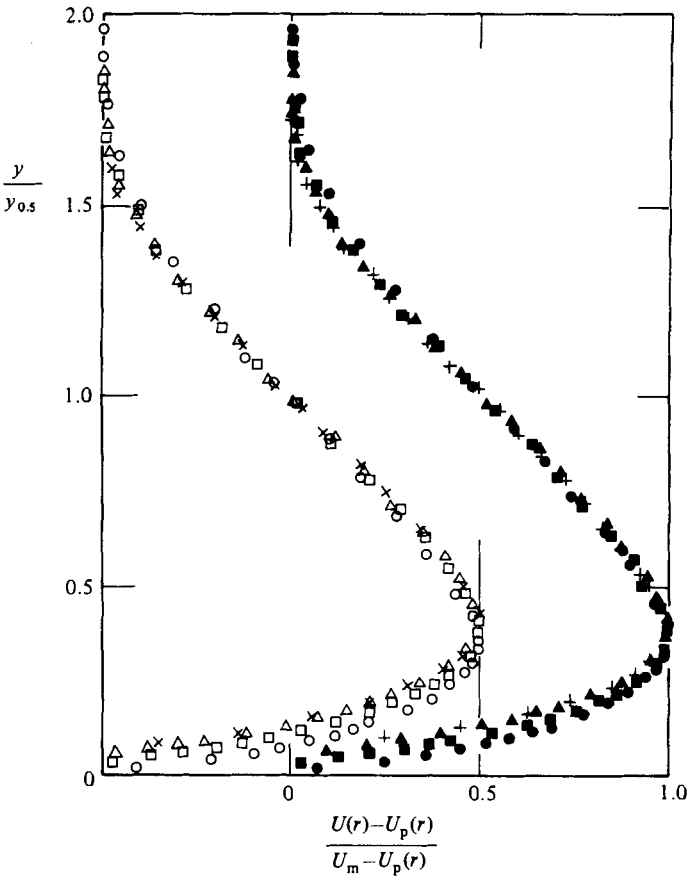

FIGURE 2. Mean-velocity profiles from pressure-tube measurements in the flat (open symbols) and curved (closed symbols) wall jets. Single hot-wire measurements at the last station are denoted by ×, +.

(figure 3) show well-defined semilogarithmic regions which have been fitted to the flat-plate boundary law of the wall

$$u^+ = \frac{1}{\kappa} \ln y^+ + A, \tag{1}$$

with $\kappa = 0.41$ and $A = 5.0$, to obtain c_f by the Clauser method. The extent of this region, up to about $y^+ = 200$, is less than that in a boundary layer but greater than that previously found in wall jets in stagnant surroundings, where, as Launder & Rodi (1981) have observed, the wall-law zone is eroded by the increasing strength with distance downstream of the outer flow relative to the wall layer. The reasonable fit to the 'universal' law over a limited distance, which has also been found by Hammond (1982), is not altogether surprising when it is appreciated that the structure of a wall jet in a moving stream is intermediate between that of the other two flows.

The temperature profiles, which are plotted in figure 4, show the corresponding slow development of the thermal layer with mild distortions due to wall curvature

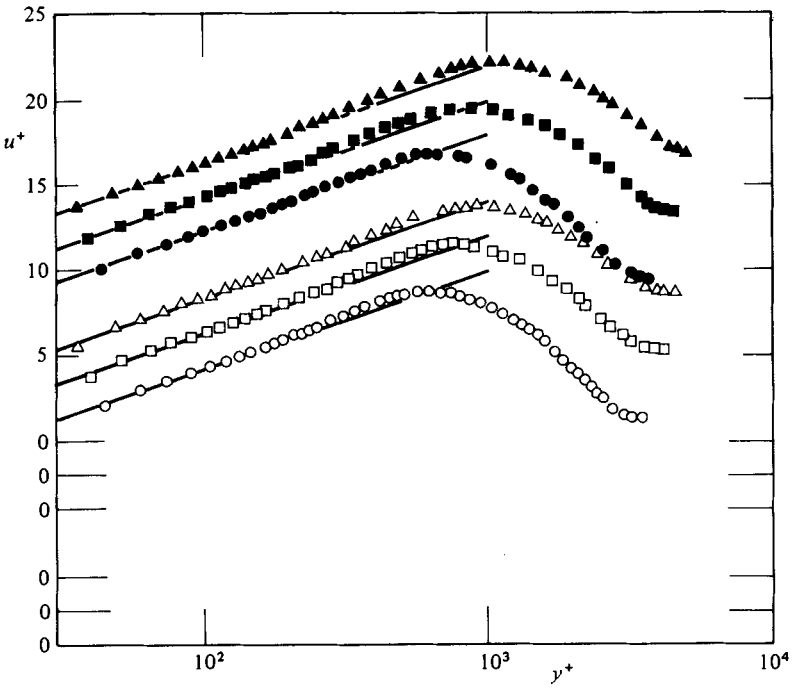

FIGURE 3. Mean-velocity profiles in wall coordinates. Lines are $u^+ = 2.44 \ln y^+ + 5.0$.

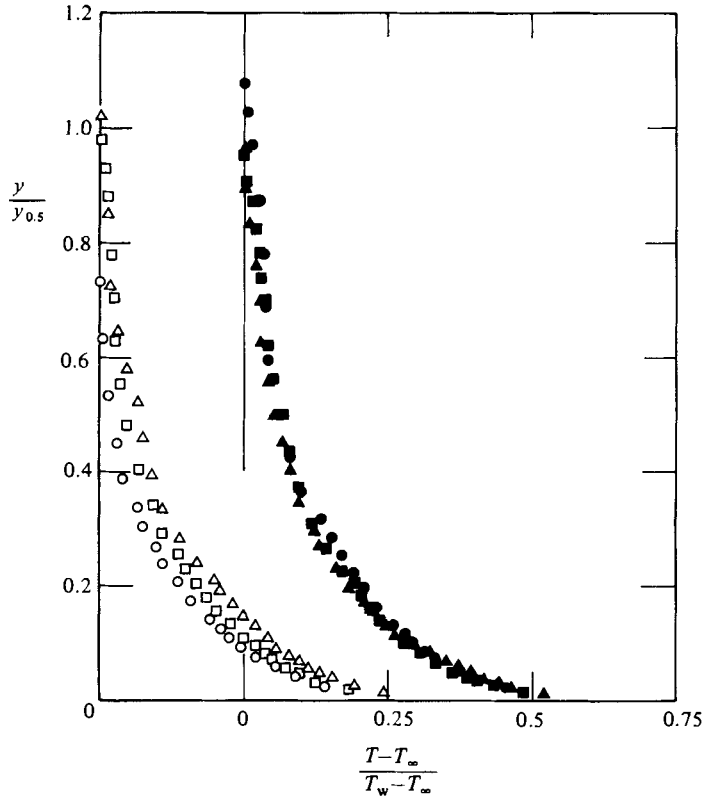

FIGURE 4. Temperature profiles in the flat and curved wall jets.

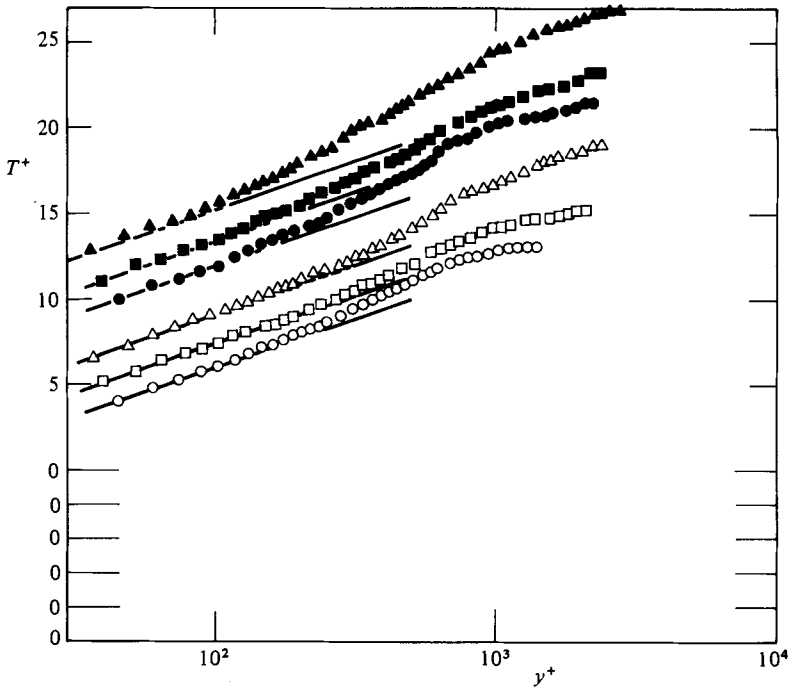

FIGURE 5. Temperature profiles in wall coordinates.

which tend to collapse the profiles. The profiles are replotted in wall-law coordinates in figure 5, where the data are compared with the usual form of the wall law

$$T^+ = \frac{\rho u_\tau c_p (T_w - T)}{q_w} = \frac{1}{\kappa_\theta} \ln \frac{y u_\tau}{\nu} + A_\theta. \tag{2}$$

In the plane flow the slopes are approximately the same for each profile, but the intercepts differ appreciably. The lines drawn in figure 5 were obtained from (2) with $\kappa_\theta = 0.4$ and $A_\theta = 4.5, 3.8, 3.6$ for $x = 46, 76, 102$ cm respectively. These values may be compared with $\kappa_\theta = 0.48$ and $A_\theta = 3.8$, recommended by Kader & Yaglom (1972) in their survey of heated boundary-layer data, and used to fit our plane boundary-layer results (Gibson *et al.* 1982). The ratio κ/κ_θ, which may be interpreted as a sort of global turbulent Prandtl number for the near-wall layer, thus has a value near unity in the plane wall jet compared to the value of about 0.85 in the plane boundary layer. The results may also be compared with Nizou's (1981) finding that the temperature profile in a plane wall jet in stagnant surroundings is fitted by (2) when $\kappa_\theta = 0.82$ and $A_\theta = 6.7$. It is not easy to account for this very substantial difference, although it may be noted that Nizou's results are associated with a wall law ($\kappa = 0.55$, $A = 8.1$) equally far from the accepted boundary-layer form which has been found (Hammond 1982) to correlate wall-jet data. The first two profiles in the curved wall jet show small but consistent departures from the plane flow results corresponding to an erosion of the inner layer, which now does not extend far beyond $y^+ = 100$. This trend is more evident in the last profile of the curved flow, where the logarithmic layer has virtually disappeared: a straight line drawn through the inner points here corresponds to $\kappa_\theta \approx 0.35$ or an increase in the 'turbulent Prandtl number' κ/κ_θ to 1.2. These changes in the curved flow are consistent with the boundary-layer results cited previously. That they are less marked in the present case is due partly to the fact that the ratio

y_s/R of inner-layer thickness to radius is but one third of δ/R in the boundary-layer experiment and partly because the dynamic response of the turbulence is different when the flow develops from effectively zero thickness on a curved wall to the response when the curvature is introduced as a sudden change in surface conditions.

3.2. *Turbulence measurements*

Profiles of the Reynolds stresses measured at the three traverse positions in both flows are plotted in figures 6 and 7, with Irwin's (1973) results from a self-preserving plane wall jet shown for comparison. The apparent large increase in turbulent intensity with downstream distance is due to the decay of the velocity deficit $U_m - U_{pw}$, which has been used to normalize the results. In absolute terms the turbulence decays as the flows develop: e.g. $\overline{uv}_{max} \times 10^3/U_j^2$ decreases from about 1.2 to 0.64 and from 1.4 to 0.8 in the plane and curved flows respectively. The results presented in this way are analogous to wake-flow data plotted similarly: self-preservation is obtained only for vanishing velocity deficit far downstream. Values of the wall shear stress obtained by the Clauser method are plotted on the ordinate of figure 7 (*a*); they are entirely consistent with the hot-wire measurements.

The intensities and shear stresses are substantially increased in the destabilized outer layer of the curved wall jet and reduced by a lesser amount in the stabilized wall layer. Significant changes are observed in the vicinity of the velocity maximum, where the turbulence is farthest from local equilibrium, the extra strain associated with curvature of the streamlines is large in comparison with the mean shear, and turbulent diffusion plays a major role in the energy and shear-stress budgets. The zero-shear-stress position y_s, which in the plane wall jet lies between $0.9y_m$ and $0.97y_m$, is displaced to about $0.7y_m$ in the curved flow. In both cases the positions of zero stress and maximum velocity are closer together than in the wall jet in stagnant surroundings, where the influence of the outer flow is relatively stronger. Irwin (1973) and Tailland (1970) located y_s at $0.6y_m$ and $0.66y_m$ respectively in their plane self-preserving wall jets; Alcaraz (1977) found y_s decreasing to about $0.4y_m$ as his curved wall jet in stagnant surroundings developed on a 16° circular arc. The positions of the minima of the normal stresses are similarly displaced in the curved wall jet. In the plane flow the minima of $\overline{u^2}$ and $\overline{w^2}$ move from just inside to just outside the maximum-velocity point as the jet spreads downstream. The minimum of $\overline{v^2}$, which does not appear in the Irwin and Alcaraz data, lies inside y_m at each of the three stations. One effect of the wall curvature is to increase the spread of these minima as well as to move them closer to the wall relative to y_m. Plane-flow behaviour is repeated in that the $\overline{u^2}$ and $\overline{w^2}$ minima appear at increasing fractions of y_m as the flow develops, but that of $\overline{v^2}$ remains at about $0.5y_m$, which is well inside y_s.

In the curved wall jet the outer layer extends effectively from the free stream to the zero-shear-stress point. The direct effects of curvature on turbulent-energy production are most apparent at $0.8y_{0.5}$ in the outer layer, where the shear stress is greatest. The extra production is in $\overline{v^2}$, where the term $4\overline{uv}U/r$ appears in the transport equation of Appendix A. The results show that $\overline{v^2}$ is increased from plane-flow levels by the greatest proportionate amount, but also that the additional energy generated in this component is very effectively redistributed to the other two components by the pressure–strain mechanism. Figure 7 (*b*) shows the effects of curvature on the structure function $\overline{uv}/\overline{q^2}$. In the inner and outer layers, where the turbulence approaches local energy equilibrium, this quantity has the values of approximately ± 0.15 that are commonly assumed in the calibration of turbulence models for boundary layers. The small but consistent increases that are observed in

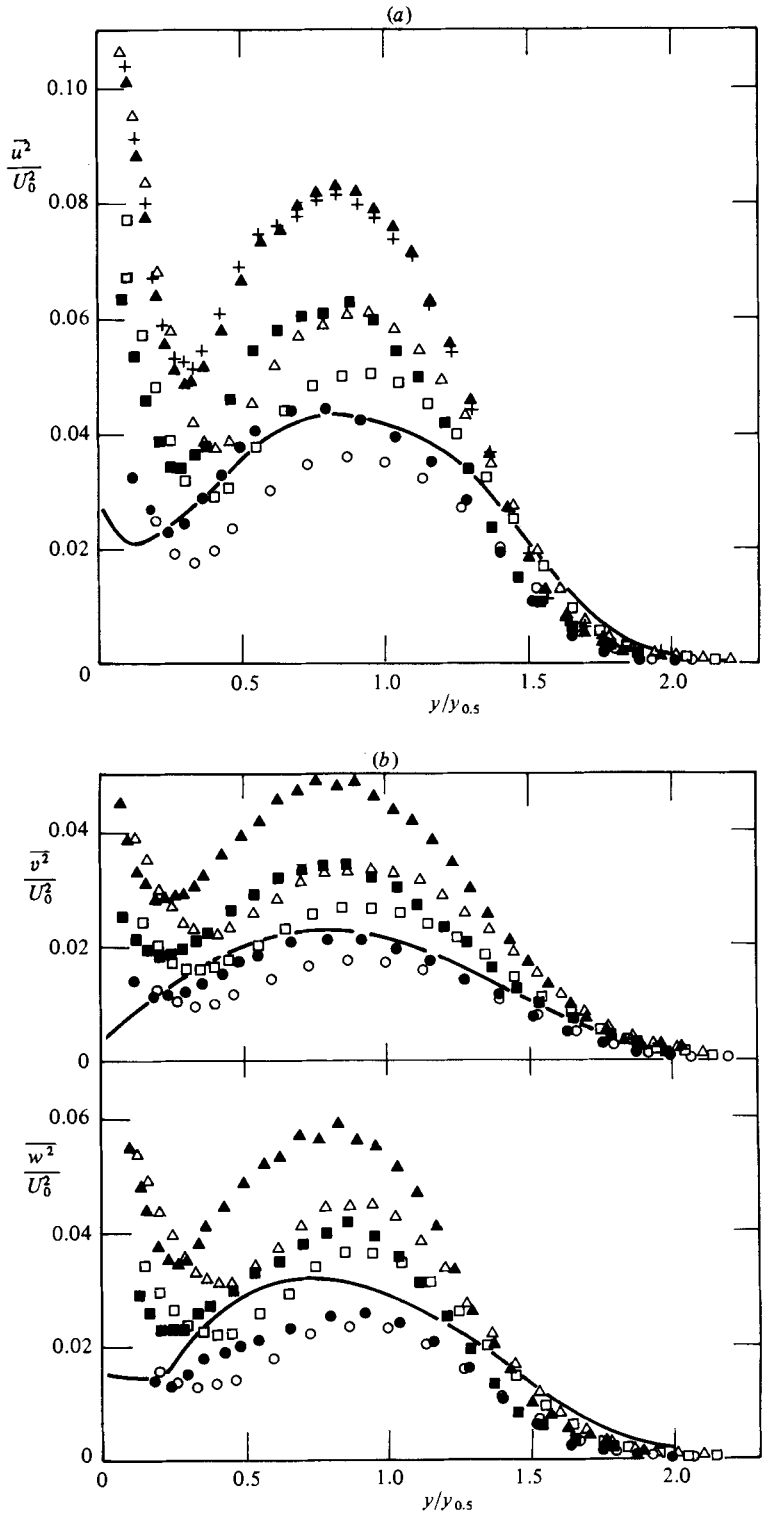

FIGURE 6. Distributions of the normal stresses normalized by $U_0^2 = (U_m - U_{pw})^2$. In (*a*) single-wire measurements of $\overline{u^2}$ at final station in curved flow are denoted by +. ——, data of Irwin (1973).

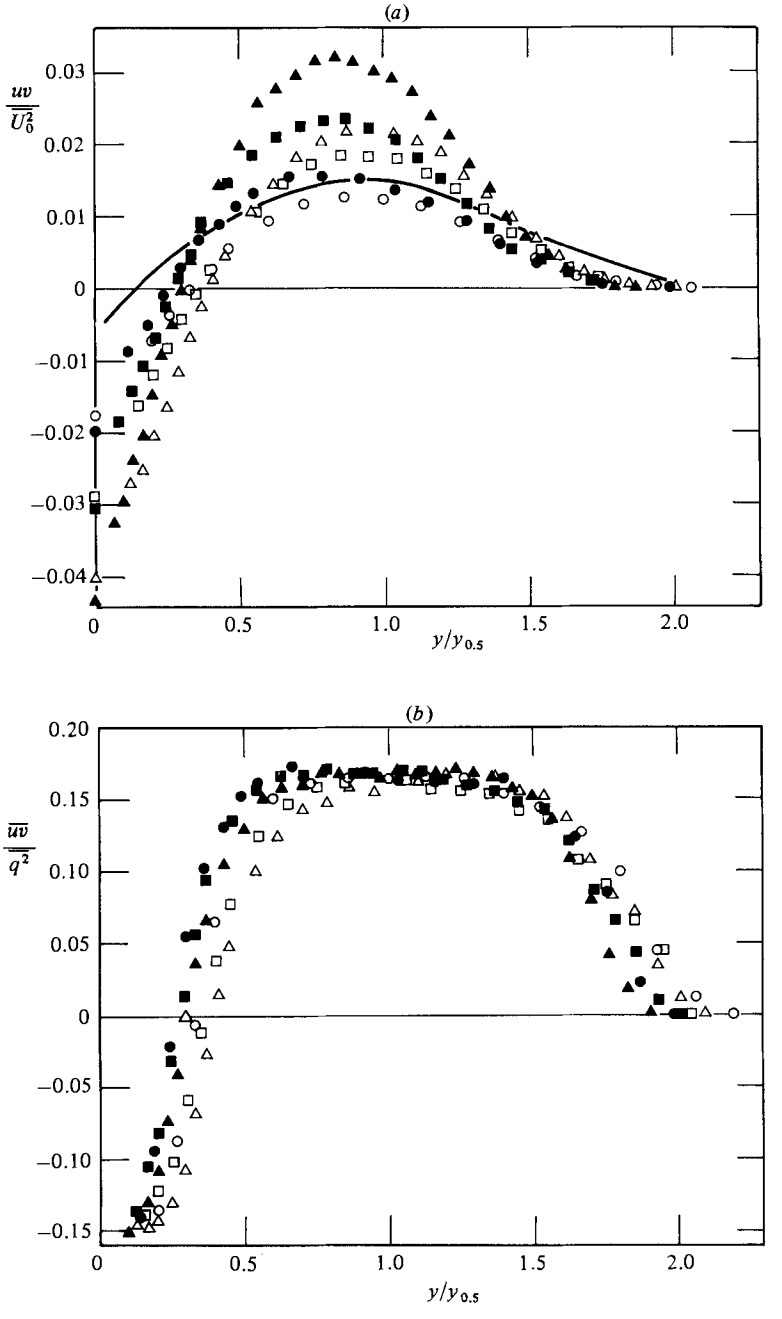

FIGURE 7. (*a*) Profiles of the shear stress compared with the data of Irwin (1973) from a self-preserving wall jet in a pressure gradient. (*b*) Distribution of the structure function $\overline{uv}/\overline{q^2}$ in flat and curved wall jets.

the curved flow away from the zero-stress zone reflect the greater sensitivity of shear stress to curvature than turbulent energy.

Measurements of temperature–velocity correlations and the temperature variance were made in each flow at the third traverse position, where the layers were thick enough to accommodate the three-wire probe. The measurements of $\overline{\theta^2}$ and $\overline{u\theta}$ were

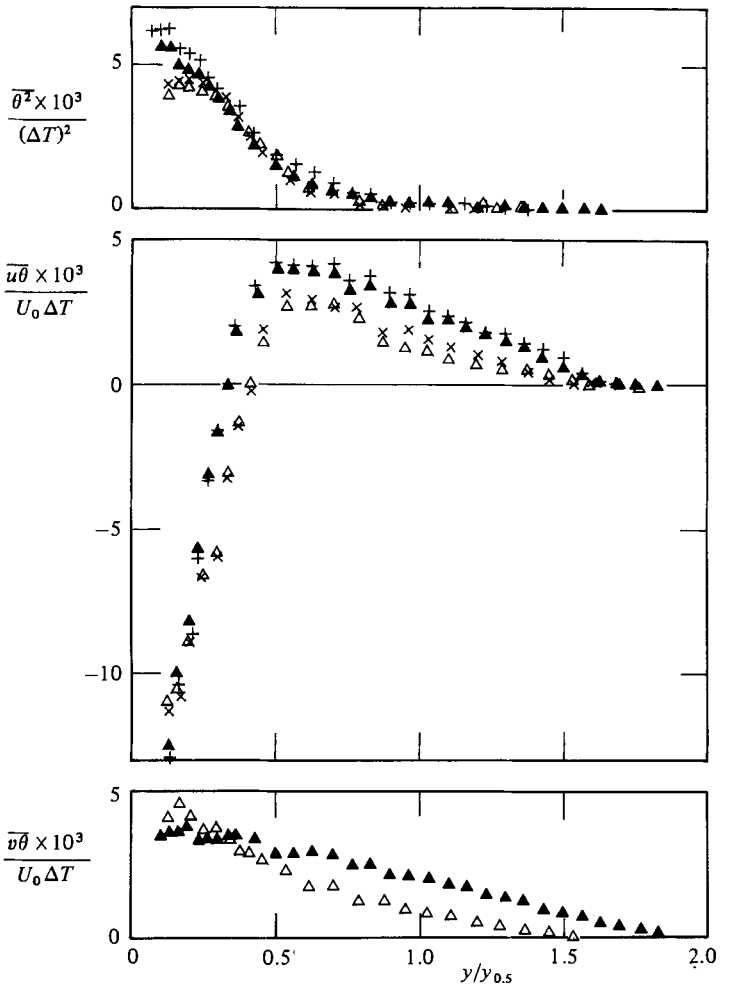

FIGURE 8. Distributions of the temperature variance, and the streamwise and cross-stream heat fluxes measured with the three-wire probe at the last station in the flat and curved flows. Twin-wire measurements of $\overline{\theta^2}$ and $\overline{u\theta}$ are denoted by $\times$, $+$. $\Delta T \equiv T_w - T_\infty$.

also checked using the parallel two-wire probe with the results shown in figure 8; the agreement is very good. Except in the inner layer, where steeper temperature gradients in the curved flow and, possibly, higher diffusion rates in the plane flow result in lower values of $\overline{\theta^2}$ in the latter, the temperature variance is not greatly affected by curvature. The marginally higher levels recorded in the destabilized outer layer are attributable to slightly increased production rates due to higher levels of $\overline{v\theta}$. The profiles of the streamwise heat flux $\overline{u\theta}$ are similar in form to the shear-stress profiles, and the changes observed in the curved flow are also qualitatively similar, most noticeably in the inward displacement of the positions of zero $\overline{u\theta}$ to, or close to, the positions of zero shear stress. In the inner layer the two dominant production terms in the transport equation (Appendix A), those that contain the mean-temperature and velocity gradients, combine to produce large negative values of $\overline{u\theta}$ near the wall. The relatively small 'apparent' production term in U/r, which results from rotation of the axes, is of the same sign and thus reinforces this trend. In the

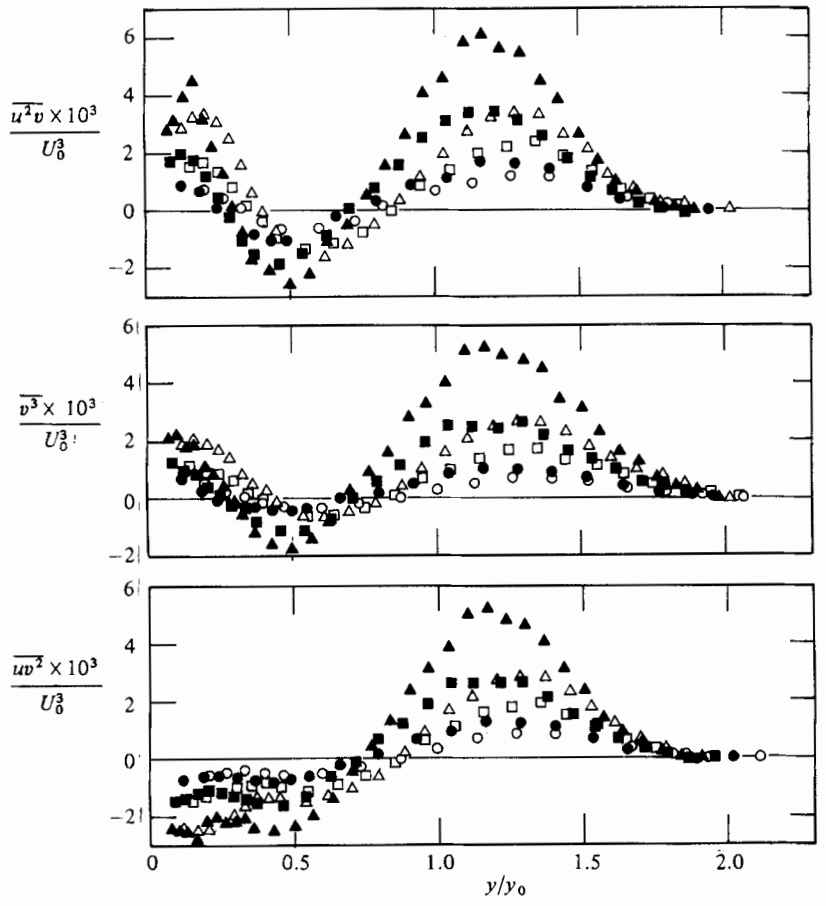

FIGURE 9. Distributions of the triple-velocity products.

outer layer the two main generation terms change sign, $\overline{u\theta}$ is positive and although the U/r term is of the opposite sign its effect is masked by increased production levels resulting from substantially higher shear stress in the destabilized outer layer. The profiles of $\overline{v\theta}$ show the presence of steep gradients near the wall. The nearest measurements were made at points about one-third of the inner-layer thicknesses from the wall. There the flux has fallen to roughly half of the wall values of 0.008 and 0.0077 recorded by the meters in the plane and curved walls respectively. Although the readings from the three-wire probe are probably low in this region, that they are well supported by the two-wire probe measurements of $\overline{\theta^2}$ and $\overline{u\theta}$ provides some basis for assuming that they are not greatly in error. The analysis by Verriopoulos (1983) of boundary-layer measurements of $\overline{v\theta}$ made with the same instrument suggests that the error here is no greater than 15%. In the outer layers, where the accuracy of the measurements is not affected by the proximity of the wall, the heat-flux levels are again raised, as expected, by the effects of destabilizing curvature.

Turbulent diffusion of turbulent energy and shear stress associated with the triple-velocity products is dominated by the large-scale motion, which is most strongly affected by longitudinal curvature. The profiles of $\overline{u^2v}$ and $\overline{v^3}$, which are plotted in figure 9, show turbulent-energy transport from the two high-shear

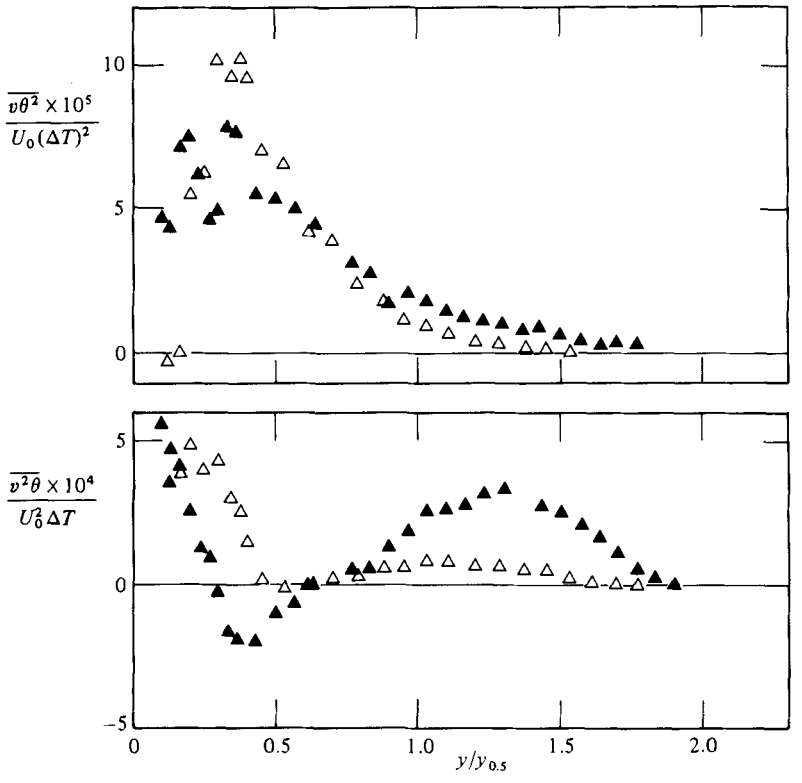

FIGURE 10. Distributions of the triple-velocity–temperature products.

high-intensity regions close to the wall in the inner layers, and at about $y/y_{0.5} = 0.8$ in the outer layers, to the regions about the zero-shear-stress positions. The triple products do in fact pass through zero at, or very close to, the zero-shear-stress points, which thus mark the divide between outward and inward energy transport. The effects of curvature on turbulent transport are most apparent in the outer layer, where peak values of the triple products are roughly doubled in the curved flow. Nevertheless the effects appear to be smaller when the curvature is destabilizing than when it is stabilizing: boundary-layer measurements (Gibson *et al.* 1984) show that convex wall curvature an order of magnitude smaller actually halved the triple products while we were unable to detect any significant changes in these quantities in a destabilized mixing layer of comparable δ/R (Gibson & Younis 1982). In the inner curved layer an attenuation of about 15 % might be expected from scaling the boundary-layer data by δ/R: changes of this order in relatively low values are obscured by unavoidable data scatter in this region. The correlation $\overline{uv^2}$, which is associated with the turbulent transport of shear stress, has a different profile shape in the inner layer (figure 9), where the shear stress is negative, but the physical interpretation is the same: outward transport of negative shear stress from the near-wall production zone and inward transport of positive shear stress from the outer-layer high-shear high-intensity region. The zero-shear-stress point again marks the boundary between these opposing processes. The contribution to the shear-stress budget in the inner layer is evidently small, as is usual in wall layers. The changes due to curvature are of the same order and in the same sense as those observed in $\overline{u^2v}$ and $\overline{v^3}$.

The results of the three-wire-probe measurements of the temperature–velocity

triple correlations made at the last traverse position are shown in figure 10. Peak values of $\overline{v\theta^2}$ appear in the vicinity of the zero-shear-stress point, and there is some indication that close to the wall $\overline{v\theta^2}$ becomes negative as in a heated boundary layer (Gibson & Verriopoulos 1984). The pattern of $\overline{\theta^2}$ diffusion is thus quite different to that of the Reynolds-stress components, with transport away from the zero-stress maximum-velocity region. The contribution to the $\overline{\theta^2}$ budget is small where the gradients of the triple-velocity products tend to be high. The profiles of $\overline{v^2\theta}$, which are also plotted in figure 10, resemble those of the triple-velocity products in being double-peaked but with relatively much higher values recorded in the inner layer. The principal changes due to curvature are, similarly, to displace the first zero of $\overline{v^2\theta}$ with the zero-shear-stress point and to stimulate $\overline{v\theta}$ transport in the destabilized outer layer.

4. Implications for turbulence modelling

The turbulent wall jet is a demanding test case for flow-calculation methods. The fact that the points of zero shear stress and zero strain do not coincide effectively rules out the use of mean-field closure methods involving simple eddy-viscosity assumptions, the more so in convex wall flow, where these points move even further apart. The problem is not insuperable, and we have been able to calculate two-dimensional wall jets on flat and curved surfaces with tolerable accuracy using a relatively uncomplicated Reynolds-stress closure method (Gibson & Younis 1982).

The problem of modelling the effects of streamline curvature on turbulent heat transfer is much more difficult. The difficulties arise at two levels: in the prediction of the effects in the fully turbulent part of the flow, and in the treatment of heat transfer through the sublayers adjacent to a curved wall. The obvious solution to the first of these would seem to be to model the pressure and triple-correlation terms of the heat-flux equations of Appendix A in much the same way as the corresponding terms in the Reynolds-stress equations. That this approach, though undoubtedly correct in principle, fails to reproduce the observed trends is almost certainly due to the use of the same length- and timescales in modelling the heat-flux and Reynolds-stress equations. The ability to calculate wall flows at all depends very largely on the existence of a universal velocity distribution near the wall. All practical calculation methods rely on wall functions derived from this universal law, and the fact that it does not change with surface curvature permits the calculation of curved wall jets and boundary layers. There now seems to be little doubt that the corresponding temperature law of the wall does change with surface curvature, and for the wall jet an additional complication is that the law is not the same as for a boundary layer. The change in one of the constants (κ_θ) in (2) may, in principle, be estimated from a suitable second-order closure model which can be used to evaluate the dependence of the turbulent Prandtl number on the curvature Richardson number in local-equilibrium turbulence. Verriopoulos (1983) has shown how the additive constant A_θ might be determined by mixing-length modifications for curved flow, but the results are not unique and the data base is far too narrow for general conclusions to be drawn with any confidence.

5. Conclusions

The measurements confirm the view that thermal turbulence in shear layers is highly sensitive to longitudinal-curvature effects. In the curved wall jet the extra resistance to heat transfer in the stabilized wall layer produces Stanton numbers lower

than plane-flow values by a greater amount than the change in skin-friction coefficient. That the response of the temperature field is radically different to that of the velocity is suggested by the finding that the temperature law of the wall is altered in curved flow in a way that the corresponding velocity law is not. In this respect the wall layer behaves in just the same way as a curved wall boundary layer; the changes due to curvature appear not to be greatly affected by the changes in the opposite sense in the destabilized outer layer. In other respects the effects of curvature are broadly in accord with expectations. The destabilized outer layer encroaches on the wall layer so as to displace the zero-shear-stress position to a point closer to the wall. Extra strain generation of turbulence results in higher intensity and stress levels in the curved outer layer, but, since the changes relative to the plane flow are not proportionately as large as those recorded in a stably curved boundary layer, it appears that destabilizing curvature is less effective than stabilizing in changing the structure of the turbulence. As has been observed in curved-boundary-layer experiments the largest proportional changes relative to plane flow are in the triple correlations associated with the turbulent transport of stress, intensity and heat flux. The pattern of turbulent diffusion in plane and curved flow is the same, and fixed relative to the zero-shear-stress position.

That the two flows are not self-preserving but develop significantly over the lengths of the test sections is no bar to the data being used to test calculation methods. The lack of self-preservation does, however, make close comparison with other wall-jet velocity-field data more difficult, although the main features of the flows and the changes due to curvature are broadly in line with expectations and consistent with earlier work. The observation that the temperature and velocity layers respond differently to curvature effects may be due to different response times in the developing flow, i.e. the time taken by changes in stress levels to effect changes in the velocity distribution may be different to the time taken by the temperature distribution to respond to changes in the heat fluxes. The thermal/mechanical time-scale ratio in boundary layers appears to be about 0.5 (Verriopoulos 1983); a quicker response by the thermal turbulence in developing flow would be consistent with the present observations.

We gratefully acknowledge financial support provided by the Science and Engineering Research Council through Grant GR/A/76634.

Appendix A. Conservation equations for curved shear layers

Transport equations for second-moment quantities in two-dimensional curved shear layers are obtainable from the equations of motion in the usual way. When, for brevity, $\mathrm{D}/\mathrm{D}t$ is written for $U\partial/\partial x + V\partial/\partial y$ and ϵ for the dissipation rate of turbulent energy (assumed in high-Reynolds-number turbulence to be equally distributed between components) and the boundary-layer approximations are made, the equations for high-Reynolds-number uniform-property flow are

$$\frac{\mathrm{D}\overline{u^2}}{\mathrm{D}t} = -\frac{\partial}{\partial y}(\overline{u^2 v}) - 2\overline{uv}\frac{\partial U}{\partial y} - \left\{2\overline{uv}\frac{U}{r}\right\} + 2\frac{\overline{p'}\overline{\partial u}}{\rho}\frac{}{\partial x} - \tfrac{2}{3}\epsilon,$$

$$\frac{\mathrm{D}\overline{v^2}}{\mathrm{D}t} = -\frac{\partial}{\partial y}\left(\overline{v^3} + \frac{\overline{p'v}}{\rho}\right) + 2\overline{uv}\frac{U}{r} + \left\{2\overline{uv}\frac{U}{r}\right\} + 2\frac{\overline{p'}\overline{\partial v}}{\rho}\frac{}{\partial y} - \tfrac{2}{3}\epsilon - 2\frac{\overline{v\theta}}{T}\frac{U^2}{r},$$

$$\frac{\mathrm{D}\overline{w^2}}{\mathrm{D}t} = -\frac{\partial}{\partial y}\overline{vw^2} + 2\frac{\overline{p'}\overline{\partial w}}{\rho}\frac{}{\partial z} - \tfrac{2}{3}\epsilon,$$

$$\frac{\mathrm{D}\overline{uv}}{\mathrm{D}t} = -\frac{\partial}{\partial y}\left(\overline{uv^2} + \frac{\overline{p'u}}{\rho}\right) - \overline{v^2}\frac{\partial U}{\partial y} + u^2\frac{U}{r} + \left\{\left(u^2 - \overline{v^2}\right)\frac{U}{r}\right\} + \frac{\overline{p'}}{\rho}\left(\frac{\overline{\partial u}}{\partial y} + \frac{\overline{\partial v}}{\partial x}\right) - \frac{\overline{u\theta}}{T}\frac{U^2}{r},$$

$$\frac{\mathrm{D}\overline{\theta^2}}{\mathrm{D}t} = -\frac{\partial}{\partial y}\overline{v\theta^2} - 2\overline{v\theta}\frac{\partial T}{\partial y} - 2\epsilon_\theta,$$

$$\frac{\mathrm{D}\overline{u\theta}}{\mathrm{D}t} = -\frac{\partial}{\partial y}\overline{uv\theta} - \overline{uv}\frac{\partial T}{\partial y} - \overline{v\theta}\frac{\partial U}{\partial y} - \left\{\overline{v\theta}\frac{U}{r}\right\} + \frac{\overline{p'}}{\rho}\frac{\overline{\partial \theta}}{\partial x},$$

$$\frac{\mathrm{D}\overline{v\theta}}{\mathrm{D}t} = -\frac{\partial}{\partial y}\left(\overline{v^2\theta} + \frac{\overline{p'\theta}}{\rho}\right) - \overline{v^2}\frac{\partial T}{\partial y} + \overline{u\theta}\frac{U}{r} + \left\{\overline{u\theta}\frac{U}{r}\right\} + \frac{\overline{p'}}{\rho}\frac{\overline{\partial \theta}}{\partial y} - \frac{\overline{\theta^2}}{T}\frac{U^2}{r}.$$

Extra production terms contain the 'extra' strain U/r associated with streamline curvature. The terms in { } also act to augment or reduce Reynolds stress or heat flux; they are not formally generation terms but appear in the equations as a result of coordinate-axis rotation.

'Centrifugal-buoyancy' sources of $\overline{v^2}$, $\overline{uv}$ and $\overline{v\theta}$ appear in the equations for heated curved flow. These are the terms in U^2/r; for the temperature differences of the present experiments they make insignificant contributions to the budgets of the dependent variables in question.

Appendix B. Momentum and enthalpy integral balances

Momentum integral balance

The integral momentum equation for flow on a uniformly curved wall can be obtained (East 1981) in the usual form

$$\frac{u_\tau^2}{U_{\mathrm{pw}}^2} = \frac{\mathrm{d}\delta_2}{\mathrm{d}x} + \left(2 + \frac{\delta_1}{\delta_2}\right)\frac{\delta^2}{U_{\mathrm{pw}}}\frac{\mathrm{d}U_{\mathrm{pw}}}{\mathrm{d}x}, \tag{A 1}$$

when small curvature terms are ignored and the displacement and momentum thicknesses are defined by

$$\delta_1 = \int_0^\infty \left[1 - \frac{U}{U_{\mathrm{pw}}} - \left(1 - \frac{U_{\mathrm{p}}}{U_{\mathrm{pw}}}\right)\right]\mathrm{d}y, \tag{A 2}$$

$$\delta_2 = \int_0^\infty \left[\frac{U}{U_{\mathrm{pw}}}\left(1 - \frac{U}{U_{\mathrm{pw}}}\right) - \frac{U_{\mathrm{p}}}{U_{\mathrm{pw}}}\left(1 - \frac{U_{\mathrm{p}}}{U_{\mathrm{pw}}}\right)\right]\mathrm{d}y. \tag{A 3}$$

As a check on the two-dimensionality of the mean flow the momentum equation is rewritten as

$$\int_{x_0}^{x} \frac{u_\tau^2}{U_{\mathrm{pw0}}^2}\mathrm{d}\left(\frac{x}{\delta_{20}}\right) = \frac{U_{\mathrm{pw}}^2\delta_2}{U_{\mathrm{pw0}}^2\delta_{20}} - 1 + \frac{1}{2}\int_{x_0}^{x}\frac{\delta_1}{\delta_{20}}\mathrm{d}\left(\frac{U_{\mathrm{pw}}}{U_{\mathrm{pw0}}}\right)^2 \tag{A 4}$$

and integrated with respect to x from the first traverse position x_0 using experimentally determined values evaluated at and faired between the traverse positions. The results of this integration, which are summarized in table 2, where PL and PR are respectively the left- and right-hand sides of (A 4), show that the flow is reasonably two-dimensional. The maximum imbalance nowhere exceeds 10%, a figure that compares favourably with the results from comparable experiments (e.g. in Coles & Hirst 1968), and gives confidence in the use of the Clauser method for evaluating u_τ in these flows.

x	Plane wall jet		Curved wall jet	
(cm)	PL	PR	PL	PR
46	0	0	0	0
66	−0.077	−0.093	−0.069	−0.065
76	−0.120	−0.137	−0.107	−0.098
91	−0.181	−0.184	−0.161	−0.147
102	−0.219	−0.204	−0.193	−0.181

TABLE 2. Momentum integral balance

x	Plane wall jet		Curved wall jet	
(cm)	TL	TR	TL	TR
46	0	0	0	0
66	0.284	0.278	0.228	0.233
76	0.363	0.372	0.336	0.351
91	0.513	0.510	0.497	0.495
102	0.610	0.595	0.597	0.570

TABLE 3. Enthalpy integral balance

Enthalpy integral balance

The integral enthalpy equation equivalent to (A 4) is

$$\int_{x_0}^{x} \frac{q_w}{[\rho c_p U_{pw}(T_w - T_\infty)]_0} \mathrm{d}\left(\frac{x}{\Delta_{20}}\right) = \frac{\rho c_p U_{pw} \Delta_2 (T_w - T_\infty)}{[\rho c_p U_{pw} \Delta_2 (T_w - T_\infty)]_0} - 1, \tag{A 5}$$

where q_w is the heat flux measured at the wall, the fluid properties ρ and c_p are evaluated at the film temperature $\frac{1}{2}(T_w + T_\infty)$, and the integral energy thickness is defined by

$$\Delta_2 = \int_0^\infty \frac{\rho c_p U}{\rho_f c_{pf} U_{pw}} \frac{T - T_\infty}{T_w - T_\infty} \mathrm{d}y. \tag{A 6}$$

Equation (A 5) is integrated from the first traverse position x_0 using the experimentally determined values. The results are summarized in table 3, and show satisfactory agreement between the left-hand (TL) and right-hand (TR) sides of (A 5).

REFERENCES

ALCARAZ, E. 1977 Contribution à l'étude d'un jet plan turbulent évoluant le long d'une paroi convexe à faible courbure. Thesis, Université de Lyon.

BRADSHAW, P. 1966 The effect of initial conditions on the development of a free shear layer. *J. Fluid Mech.* **26**, 225.

BRADSHAW, P. 1969 The analogy between streamline curvature and buoyancy in turbulent shear flow. *J. Fluid Mech.* **36**, 177.

BRADSHAW, P. 1973 Effects of streamwise curvature on turbulent flow. *AGARDograph* 169.

COLES, D. C. & HIRST, E. A. 1968 Computation of turbulent boundary layers. In *Proc. AFOSR–IFP–Stanford Conf*, vol. 2, p. 47.

EAST, L. F. 1981 A representation of second-order boundary layer effects in the momentum integral equation and in viscous–inviscid interactions. *RAE TR* 81002.

GIBSON, M. M. 1978 An algebraic stress and heat flux model for turbulent shear flow with streamline curvature. *Intl J. Heat Mass Transfer* **21**, 1609.

GIBSON, M. M., VERRIOPOULOS, C. A. & NAGANO, Y. 1982 Measurements in the heated turbulent boundary layer on a mildly curved convex surface. In *Turbulent Shear Flows* 3 (ed. L. J. S. Bradbury, F. Durst, B. E. Launder, F. W. Schmidt & J. H. Whitelaw), p. 80. Springer.

GIBSON, M. M. & VERRIOPOULOS, C. A. 1984 Turbulent boundary layer on a mildly curved convex surface: II, Temperature field measurements. *Expts Fluids* **2**, 73.

GIBSON, M. M., VERRIOPOULOS, C. A. & VLACHOS, N. S. 1984 Turbulent boundary layer on a mildly curved convex surface: I, Mean flow and turbulence measurements. *Expts Fluids* **2**, 17.

GIBSON, M. M. & YOUNIS, B. A. 1982 Modelling the curved turbulent wall jet. *AIAA J.* **20**, 1707.

GIBSON, M. M. & YOUNIS, B. A. 1983 Turbulence measurements in a developing mixing layer with mild destabilizing curvature. *Expts Fluids* **1**, 23.

GUITTON, D. E. & NEWMAN, B. G. 1977 Self-preserving turbulent wall jets over convex surfaces. *J. Fluid Mech.* **81**, 155.

HAMMOND, G. P. 1982 Complete velocity profile and optimum skin friction formulae for the plane wall jet. *Trans. ASME* I: *J. Fluids Engng* **104**, 59.

IRWIN, H. P. A. H. 1973 Measurements in a self-preserving plane wall jet in a positive pressure gradient. *J. Fluid Mech.* **61**, 33.

KACKER, S. C. AND WHITELAW, J. H. 1971 The turbulence characteristics of two-dimensional wall-jet and wall-wake flows. *Trans. ASME* E: *J. Appl. Mech.* **38**, 7.

KADER, B. A. & YAGLOM, A. M. 1972 Heat and mass transfer laws for fully turbulent wall flows. *Intl J. Heat Mass Transfer* **15**, 2329.

KREITH, F. 1955 The influence of curvature on heat transfer to incompressible fluids. *Mech. Engng* **77**, 265.

KRUKA, V. & ESKINAZI, S. 1964 The wall jet in a moving stream. *J. Fluid Mech.* **20**, 555.

LAUNDER, B. E. & RODI, W. 1981 The turbulent wall jet. *Prog. Aerospace Sci.* **19**, 81.

MAYLE, R. E., BLAIR, M. F. & KOPPER, F. C. 1979 Turbulent boundary layer heat transfer on curved surfaces. *Trans. ASME* C: *J. Heat Transfer* **101**, 521.

NIZOU, P. Y. 1981 Heat and momentum transfer in a plane turbulent wall jet. *Trans. ASME* C: *J. Heat Transfer* **103**, 138.

SARIPALLI, K. R. & SIMPSON, R. L. 1980 Investigation of blown boundary layers with an improved wall jet system. *NASA CR* 3340.

SIMON, T. W. & MOFFAT, R. J. 1979 Heat transfer through turbulent boundary layers – the effects of introduction of and recovery from convex curvature. *ASME Paper* 79–WA/GT-10.

SIMON, T. W., MOFFAT, R. J., JOHNSTON, J. P. & KAYS, W. M. 1980 Turbulent boundary layer heat transfer experiments: convex curvature effects including introduction and recovery. *Stanford Mech. Engng Rep.* HMT-32.

TAILLAND, A. 1970 Contribution à l'étude d'un jet plan dirigé tangentiellement à une paroi plane. Thesis, Université de Lyon.

THOMANN, H. 1968 Effect of streamwise wall curvature on heat transfer in a turbulent boundary layer. *J. Fluid Mech.* **33**, 283.

VERRIOPOULOS, C. A. 1983 Effects of convex surface curvature on heat transfer in turbulent flow. Ph.D. thesis, Imperial College.